Design of a Modular Knee-Ankle-Foot-Orthosis Using Soft Actuator for Gait Rehabilitation

S.M. Mizanoor Rahman(✉)

Department of Mechanical Engineering,
Vrije Universiteit Brussel (VUB), Pleinlaan 2, 1050 Brussels, Belgium
mizansm@hotmail.com

Abstract. The design of a modular wearable knee-ankle-foot-orthosis (KAFO) using novel soft actuator for post-stroke gait rehabilitation is presented. The configuration, different modules, working principles, actuation, control concepts, novel features etc. of the KAFO are introduced. As the actuation method plays the key role for the overall performances of the KAFO, the design, configuration, working principles, kinematics, dynamics, control analyses etc. of a novel soft actuation system are presented in details. The novel actuator is a variable impedance series elastic actuator designed with one motor and two types of springs in series, which is light in weight and compact in size. The actuator model is simulated for various conditions, and the results show satisfactory dynamic performances in terms of stability, safety, force bandwidths, variable impedance, compliance, efficiency etc. Then, the fabrication of the physical KAFO and its clinical validation with stroke patients are emphasized.

Keywords: Knee-ankle-foot-orthosis · Gait · Rehabilitation · Stroke · Modular · Soft actuator · Variable impedance · Passive compliance · Adaptive shared control · HRI

1 Introduction

1.1 Severity of Stroke Diseases in the Global Perspective

According to the World Health Organization (WHO), over 5.7 million people die every year in the world due to stroke, and this number may increase to about 24 millions by 2030 [1]. Over 700,000 people per year suffer a stroke in the USA, and more than half of them survive with disability [2]. Each year, there are over 920,000 stroke cases in Europe [3]. For Australia, stroke is the second single greatest cause of death [4]. It is the leading cause of long-term disability in adults in Australia, which represents 25 % of all chronic disabilities [5]. Stroke still remains the third most common cause of death in Japan [6]. Stroke causes deaths and disabilities, it increases health care anxieties, rehabilitation and health care supports and costs [2].

A. Natraj et al. (Eds.): TAROS 2013, LNAI 8069, pp. 195–209, 2014.
DOI: 10.1007/978-3-662-43645-5_21,

1.2 Therapy for Stroke Rehabilitation: Manual vs. Robotic

Stroke damages neurons, which can only be repaired by repeated therapies. Stroke patients receiving frequent and repeated physical therapies have much greater chance of recovery than other forms of treatments [7, 8]. Repeated physical therapies can establish new neural pathways or can unmask the dormant pathways that control the volitional movement, and thus it can maximize the motor performances and minimize the functional deficits [9]. For manual physical therapy, one or more therapists assist and encourage the patient to follow a number of repetitive movements. However, the manual rehabilitation is not precise, it is slow and non-reproducible, and it adds burdens to the therapists. The repetitive nature of the stroke therapy makes it possible to provide the therapy by robots that may reduce the burden of the therapists or may replace the therapists and can measure the data on the patients while training them and thus can help record the patient's progress [2]. It is highly reproducible and precise, it ensures consistency in therapy [10]. This is why, robot-assisted therapies for the patients suffering from stroke, paralysis, cerebral palsy, paraplegic disease, polio, hemiplegic problems etc. have become very active areas of research [10–18].

1.3 Robot-Assisted Therapies for Stroke Rehabilitation: The State-of-the-Art

Rehabilitation robots for gait [10–16] and arm training [17, 18] have been developed. However, the gait training seems to be more important, but it is complicated due to the complex biomechanics of the human leg. Most of the current gait systems are set on treadmill [13], which is not natural. The existing lower limb systems usually do not have powered ankle joint [10] (except in few systems e.g. [12]). These systems are not so robust to adapt with changing environments. The existing systems are in generally expensive, large, heavy and do not include body-weight supports. Balance is not so good. Sizes have not been generalized to accommodate the patients of different sizes, ages, shapes etc. Again, most of the systems cannot provide patient's up-down, left-right, and front-back motions.

It is true that some existing systems are addressing the above issues. For example, a body weight support was proposed in [19]. Several gait trainers can be adjusted to the anatomic dimensions of the patients [10, 15]. Some systems allow actuated hip and knee flexion, actuated forward-backward motion, actuated abduction/adduction etc. [10]. However, proper integration of all the aforementioned required attributes in a single system has not been attempted yet.

1.4 Modular Design of Robotic Systems for Stroke Rehabilitation Therapy

Integrated robotic rehabilitation systems are usually larger than the particular requirement of the patients, and hence some of the facilities may remain unused. Again, these systems are usually heavy and costly. A large system may create local effects on the unexercised limbs or muscle groups of the patients. These problems motivated towards the modular design where different groups of muscles (e.g. spatial arm movements), limbs (e.g. wrist, fingers, legs) etc. are exercised separately [2, 9]. However, most of the systems do not provide modular design advantages [10–18].

The ankle plays a central role in the normal gait; it contributes to propulsion, shock-absorption and balance. The foot-drop disease due to stroke occurs in the ankle [9]. However, the present systems either do not include powered ankle-foot orthosis or the orthosis is powered but it runs on treadmill instead of over ground [10]. Again, a combined knee-ankle-foot system with modular operations of both ankle and knee modules as well as with all other required attributes are usually not seen.

1.5 Soft and Compliant Actuation for Rehabilitation Systems

The rehabilitation systems should have low friction, low and variable mechanical impedance, it should be back-drivable etc. to resemble its natural counterparts [20–23]. However, the present systems do not fully satisfy these requirements due to their limitations in their actuator systems that are not so soft, compliant and they do not provide variable impedance [7, 9]. As a results, most of the present systems are not so safe and human-friendly [2, 9–18, 24]. On the other hand, several soft, compliant and variable impedance actuators have been proposed [23, 25–32]. But, their applications in the design of the rehabilitation systems are not so satisfactory [10–18, 25, 33, 34].

1.6 Objectives

This paper presents the design, various modules, working methods, actuation, control concepts etc. of a novel wearable modular KAFO, and attempts to bring novelties in every sphere of the design so that it can overcome the limitations of the present gait rehabilitation systems. The novel variable impedance compliant series elastic actuator design for the KAFO is presented with detailed dynamic and control analyses. Then, the fabrication and clinical validation of the KAFO are emphasized.

2 Configuration of the Proposed Gait Rehabilitation System

The novel gait rehabilitation system is designed in its two different wearable modules: (i) the ankle module - a powered Ankle-Foot Orthosis (AFO) for rehabilitation and assistance at the ankle as shown in Fig. 1(a) [9], (ii) the Knee-Ankle-Foot-Orthosis (KAFO) module that has functionalities and motion generation capabilities at both knee and ankle simultaneously or independently for gait rehabilitation as shown in Fig. 1(b). The complete KAFO to use in the rehabilitation sessions is shown in Fig. 1(c), which includes a body-weight support and an omni-directional mobile base.

The kinematic analysis for the AFO as a representative of the whole KAFO based on Fig. 2 may help understand how the AFO will be actuated during the rehabilitation sessions [9]. In Fig. 2, a is shank length, b is foot length and x is linear displacement of the actuator output. The kinematics for the AFO can be described using Eq. (1).

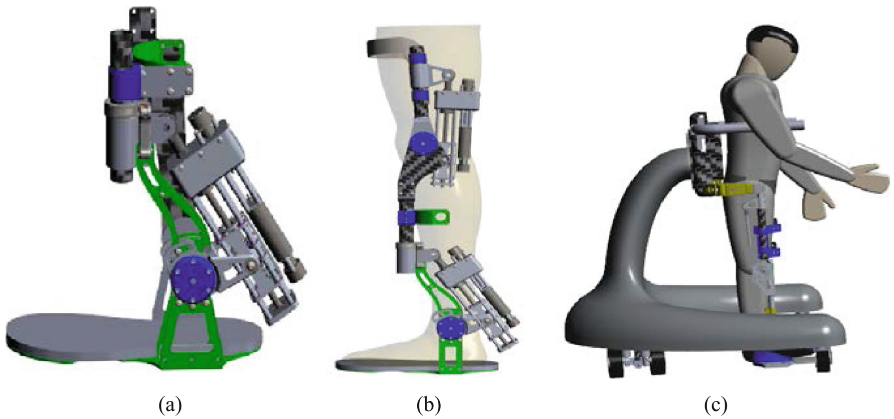

Fig. 1. (a) The AFO module, (b) the KAFO module, (c) the complete rehabilitation system.

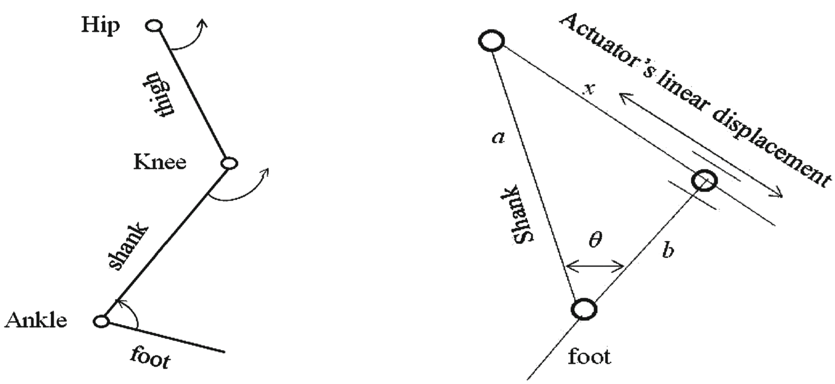

Fig. 2. Link-segment model for the kinematic analysis for the KAFO (left), and kinematic model for the AFO for the ankle-foot motion (right).

The actuator produces x, and θ changes due to the change in x. Hence, the relationship between x and θ can be established as Eq. (2). The objective is to control θ (and its derivatives) for the ankle-foot motion to assist the rehabilitation task.

The design uses carbon fiber composite material for its main structure and space grade aluminum alloy for the actuator that make it light-weight, strong and convenient [34]. A novel variable impedance compact compliant series elastic actuator (SEA) is designed for the system. The aim is to use a novel adaptive shared force control that also includes on-line learning for the adaptation to the individual patient characteristics at different stages/modules of the rehabilitation process [35]. The KAFO interface is to adapt to patient's cognitive and physical functionalities and ensure bilateral communication between them. It is also an aim to justify the design through the clinical validation of the system using the stroke patients.

$$x^2 = a^2 + b^2 - 2ab\cos\ \theta \tag{1}$$

$$\theta = f(x) \tag{2}$$

3 Novel Compliant Actuator Design for the Rehabilitation System

3.1 Novel Actuator Design

A novel SEA is designed to provide variable impedance to the lower limb system. The actuator design consists of (i) a servomotor, (ii) two springs, (iii) a ball screw and (iv) an output link. The design places a torsional spring in series between the servomotor and the ball screw. The nut of the ball screw is attached to the output link in series through another set of translational springs (see Fig. 3(a)). The servomotor with

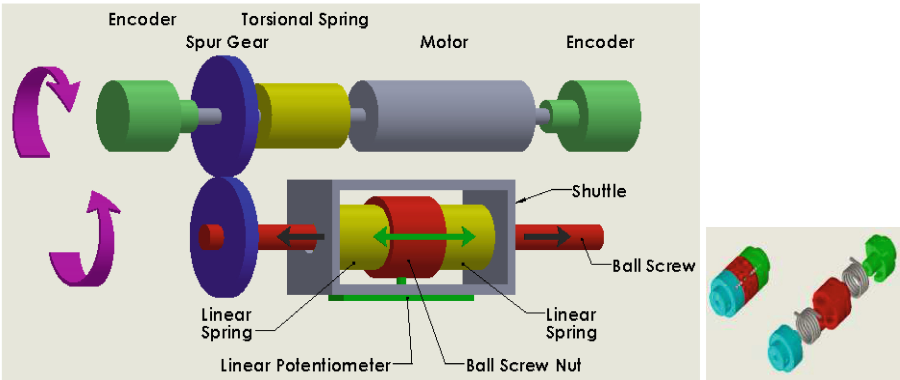

(a)

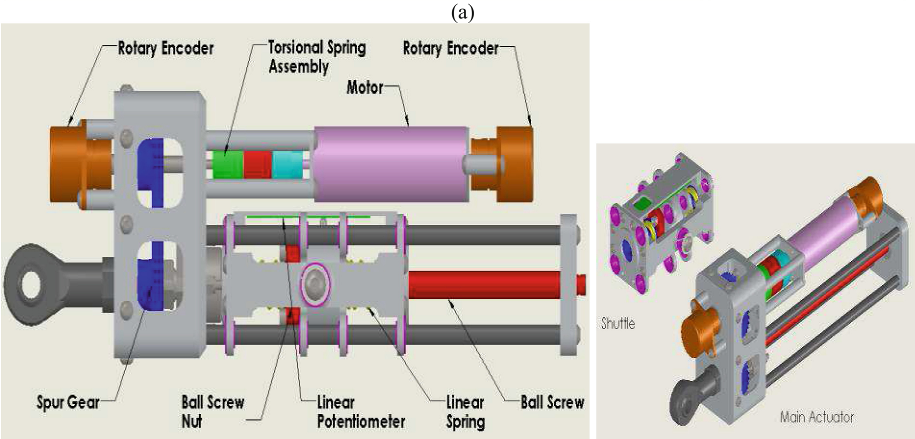

(b)

Fig. 3. (a) Mechanism of the actuator, and (b) components of the actuator with the exploded view.

an encoder is attached to the torsional spring that is attached to a spur gear and the gear is attached to another rotary encoder. The rotary encoders are used to measure the deflection of the torsional spring, and the motor torque is calculated based on the spring constant. The gear is then attached to the ball screw. The rotational speed is reduced based on the appropriate gear ratio [34, 36].

A set of translational springs is attached to the ball screw nut. If the nut moves, a deflection is created in the springs that can be measured by a linear encoder. The output force is calculated based on the spring constant and the linear deflection following the Hooke's law. The shuttle assembly is connected to the other end of the joint. The linear springs added on both ends of the ball screw nut are connected to the shuttle that can help achieve back-drivable actuation in the green-colored arrow directions. The ball screw nut can move independent of the shuttle. The key components of the force feedback are the torsional spring and two high resolution rotary encoders. The torsional spring is incorporated with a predefined spring constant and the encoders are used to measure the rotational difference between the motor (input) and the spur gear (output). To achieve the bi-directional loading of the torsional spring, it is packaged inside an assembly containing two opposite winding torsional springs loaded independently with respect to the rotational direction as it is shown in Fig. 3(a). Figure 3(b) shows the components of the actuator. An output pin is used to attach it to the output link. A hinge point is used to tie the actuator to any suitable frame of the robotic system. The translational springs are soft and small. Although the spring constant is very big, the size of the torsional spring is very small as it is at the high speed and low torque range [23, 31, 32].

The actuator main parts are designed to be machined out of aluminium (6061T6) taking the advantage of mechanical properties of the material (weight and strength). The shuttle assembly and the ball screw nut share the same linear guide for the constraint in the movement other than in the intended stroke direction. The selected motor (Maxon DC brushless motor, EC 4-pole 120 W 36 V) is universal in all joints. It is used due to its light-weight (0.175 kg), favorable power to weight ratio, low moment of inertia, and compactness. The actuator is designed to be able to provide up to 60 N m assistive torque at human joints [10, 21, 22]. In order to have a high resolution force sensing, a minimum of 1024 ppr rotary encoder is used. For mechanical transmission, the ball screw is used for high efficiency, and the spur gears are used to get the actuator compact. The ball screw is selected from Eichenberger Gewinde AG and it can output up to 1500 N force. The translational springs have a working stroke of 12 mm. These are used to operate in the range of about 25 % of the full force. Total mass of the actuator is less than 0.85 kg.

3.2 Working Principles of the Novel Actuator

To analyze the actuator performances at the output end (robot link) that produces linear output force, the actuator is modelled as a system consisting of translational elements only by converting the rotary elements to the equivalent translational elements as in Fig. 4(a). In the model, F_1 indicates motor input force, m_1 is equivalent

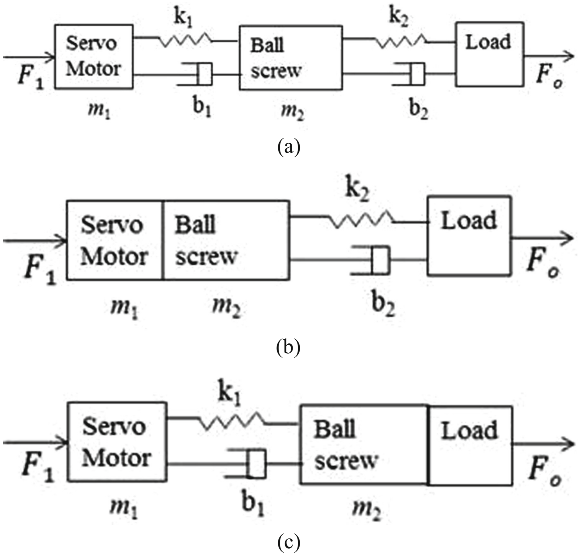

Fig. 4. (a) Working principle of the series elastic actuator for the equivalent translational motion, (b) principle for low force, (c) principle for high force case.

mass of the motor as derived in Eq. (3) where J_1 indicates moment of inertia of the motor, p indicates pitch of the ball screw, m_2 indicates equivalent mass of the ball screw as derived in Eq. (4) where J_2 indicates moment of inertia for the ball screw, k_1 indicates the equivalent translational spring constant of the torsional spring k_t as derived in Eq. (5), k_2 indicates spring constant of the translational spring, b_1 and b_2 indicate viscous damping for motor and ball screw respectively, and F_o indicates the output force. k_1 is selected to be much bigger than k_2.

At low force rehabilitation cases, the model can be reduced to as in Fig. 4(b). It means that the torsional spring is to behave as rigid and not to work as a spring, and only the translational spring is to work. Hence, the output impedance and compliance are to be produced due to only the translational spring and they are to depend on the spring constant k_2. As the allowable stroke for the translational springs is small, at high force during the rehabilitation, the translational springs are to compress and only the torsional spring is to work, thus the model is to reduce to as in Fig. 4(c). Hence, the bandwidth of the actuator is found very high at the high force cases during the rehabilitation due to big spring constant k_1. Therefore, the performances are to depend on the force range during the rehabilitation and on the difference between the spring constants k_1 and k_2. Thus, the actuator can change its output impedance and dynamic bandwidth in accordance with the force range without needing a change in the springs (hardware). The actuator thus can achieve a low output impedance and small non-linear friction because of the soft translational springs. These are also the requirements of a stroke rehabilitation robot [3, 6, 16].

3.3 The Dynamics Model for the Novel Actuator

Dynamic performances for the low (Fig. 4b) and the high (Fig. 4c) force situations are discussed as follows. The closed-loop model of the actuator is presented in Fig. 5. The dynamic motion equations are derived for the low force as in Eqs. (6)–(8) based on Figs. 4(b) and 5. If the required output force is small, the high stiffness torsional spring, motor and the ball screw may be considered as a single mass equivalent to $m_1 + m_2$. F_2 refers to the force on the translational spring k_2 and it may be calculated by the Hooke's law as Eq. (7). It is the output force on the load. x_1, x_2, x_3 are the displacements as in Fig. 5. The transfer functions based on Eqs. (6)–(8) for three conditions are derived as the following: (i) open loop transfer function with the load end fixed as in Eq. (9), (ii) closed loop transfer function with the load end fixed as in Eq. (10), and (iii) output impedance with the load end free as in Eq. (11), where F_d indicates the desired force. A PD controller expressed as $k_p + k_d.s$ is used, where k_p and k_d indicate the proportional and the derivative gain respectively. These three transfer functions completely describe the linear dynamic characteristics of the actuator [23].

$$m_1 = J_1\left(\frac{2\pi}{p}\right)^2 \tag{3}$$

$$m_2 = J_2\left(\frac{2\pi}{p}\right)^2 \tag{4}$$

$$k_1 = k_t\left(\frac{2\pi}{p}\right)^2 \tag{5}$$

$$F_1 = b_2(\dot{x}_2 - \dot{x}_3) + k_2(x_2 - x_3) + (m_1 + m_2)\ddot{x}_2 \tag{6}$$

$$F_2 = k_2(x_2 - x_3) \tag{7}$$

$$(F_d - F_2) \cdot (k_p + k_d s) = F_1 - F_2 \tag{8}$$

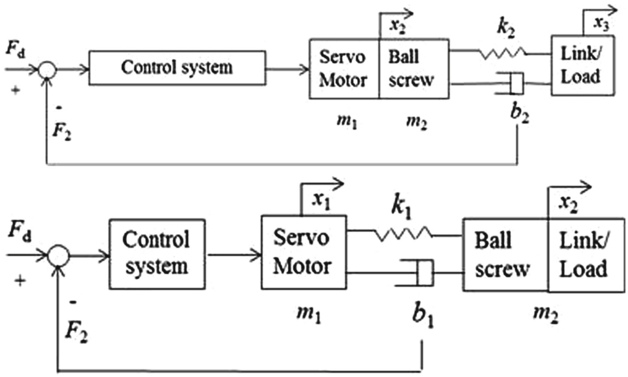

Fig. 5. Closed-loop control model of the actuator for the low (upper) and the high (lower) force situations.

$$\frac{F_2(s)}{F_1(s)} = \frac{k_2}{(m_1 + m_2)s^2 + b_2 s + k_2} \tag{9}$$

$$\frac{F_2(s)}{F_d(s)} = \frac{k_d k_2 s^2 + k_p k_2 s}{(m_1 + m_2)s^3 + b_2 s^2 + k_d k_2 s^2 + k_p k_2 s} \tag{10}$$

$$\frac{F_2(s)}{x_3(s)} = \frac{-(m_1 k_2 + m_2 k_2)s^3}{(m_1 + m_2)s^3 + b_2 s^2 + k_d k_2 s^2 + k_p k_2 s} \tag{11}$$

If the output force is large, the low stiffness spring is to be compressed completely and the ball screw and the load are to be integrated as a single mass. So, the actuator may be activated at this condition by the torsional spring only. The dynamic equations for the high force situations are derived in accordance with Figs. 4(c) and 5 as in Eqs. (12)–(15). The transfer functions for the open loop and the closed loop force control, and the output impendence are derived as in Eqs. (16)–(18) respectively.

$$m_1 \ddot{x}_1 = F_1 - k_1(x_1 - x_2) - b_1(\dot{x}_1 - \dot{x}_2) \tag{12}$$

$$m_2 \ddot{x}_2 = -k_1(x_2 - x_1) - b_1(\dot{x}_2 - \dot{x}_1) \tag{13}$$

$$F_2 = k_1(x_1 - x_2) \tag{14}$$

$$F_1 - F_2 = (F_d - F_2) \cdot (k_p + k_d s) \tag{15}$$

$$\frac{F_2(s)}{F_1(s)} = \frac{k_1}{m_1 s^2 + b_1 s + k_1} \tag{16}$$

$$\frac{F_2(s)}{F_d(s)} = \frac{k_d k_1 s + k_p k_1}{m_1 s^2 + b_1 s + k_d k_1 s + k_p k_1} \tag{17}$$

$$\frac{F_2(s)}{x_2(s)} = \frac{-m_1 k_1 s^2}{m_1 s^2 + b_1 s + k_d k_1 s + k_p k_1} \tag{18}$$

3.4 Dynamic Responses and Control Analysis for the Actuator Model

The values of m_1, m_2, b_1, b_2, k_1, and k_2 are used for MATLAB simulation for the model based on the proposed physical actuator (Table 1) for the control shown in Fig. 5. The step responses are shown in Fig. 6(a) for the small (100 N) and in Fig. 6(b) for the large (1000 N) force situations. For the small force, the PD controller's parameters are $k_\mathrm{p} = 2.1$, $k_\mathrm{d} = 0.03$ and the figure shows that the overshoot is 0 % and the settling time is 0.08 s. For the large force, the PD controller's parameters are $k_\mathrm{p} = 0.16$, $k_\mathrm{d} = 0.0003$. The overshoot is almost zero (max 2 %) and the settling time is about 0.01 s. The results thus show satisfactory dynamic performances of the design [36]. However, the control needs to be designed in such a way that a switch occurs automatically during the transformation of the system from the low to the high output force condition based on the situation or demand, and the system is also stable during the switch.

Table 1. Actuator design parameters and their values used for MATLAB simulation

Values of the actuator hardware parameters for the rotational motion	Values of the actuator hardware parameters for the equivalent translational motion
$J_1 = 8.91 \times 10^{-7}$ kg m^2	$m_1 = J_1\,(2\pi/p)^2 = 8.78$ kg
$J_2 = 642 \times 10^{-9}$ kg m^2	$m_2 = J_2\,(2\pi/p)^2 = 6.33$ kg
Torsional spring constant (k_t) = 1 N m/rad	$k_1 = k_t\,(2\pi/p)^2 = 9.86 \times 10^6$ N/m $k_2 = 24 \times 10^3$ N/m
$k_2 = 24 \times 10^3$ N/m	$b_1 = 800$ N s/m
Pitch of the ball screw (p) = 2×10^{-3} m	$b_2 = 1000$ N s/m

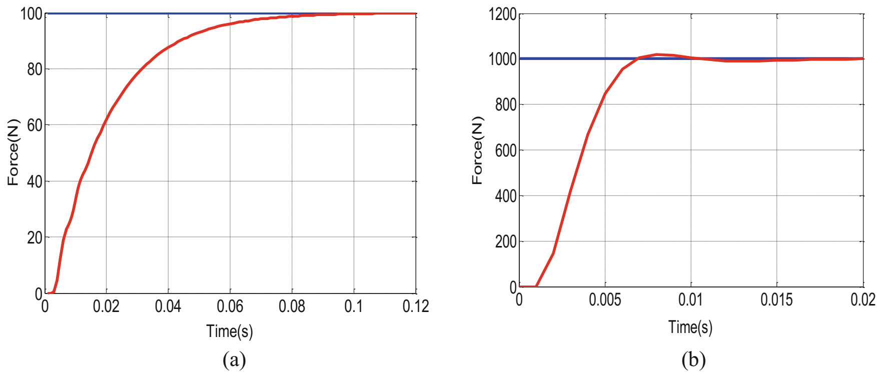

Fig. 6. Step responses for the actuator design for (a) low force (100 N), and (b) high force (1000 N) situation.

The ramp response for the actuator when both k_1 and k_2 are active is in Fig. 7. Here, the actuator performances can be checked when it transits from low to high force situation. Figure 7(a) shows almost no tracking error for both the low and the high force. The magnified graph for the point when the system enters into the high force condition (>240 N) from the low force condition (≤240 N) is shown in Fig. 7(b). The figure also shows a small tracking error (less than 5 %) when the switch occurs. The results indicate that the switch in the system control from the low to the high force is justified and there will have no tracking error, oscillations, instability etc. during the switch in the practical applications with the rehabilitation robot [36].

Bode plots for low and high force are shown in Fig. 8. For low force, the bandwidth is about 100 rad/s (16 Hz). If k_p increases the bandwidth increases, but if b_1 increases the bandwidth may decrease. There may have a possibility of resonance after 1500 rad/s (240 Hz) though the magnitude (dB) is not so high. This resonance is brought by k_1, but k_1 no longer acts as a spring for low force. In this case, the system falls within high frequency (and also high force), and hence the resonance cannot occur. For high force as in Fig. 8(b), the bandwidth is about 400 rad/s (64 Hz), and there is no possibility of resonance up to this range. This bandwidth is determined by the natural frequencies of the system as in Eq. (19) and Eq. (20), where ω_{n1} and ω_{n2}

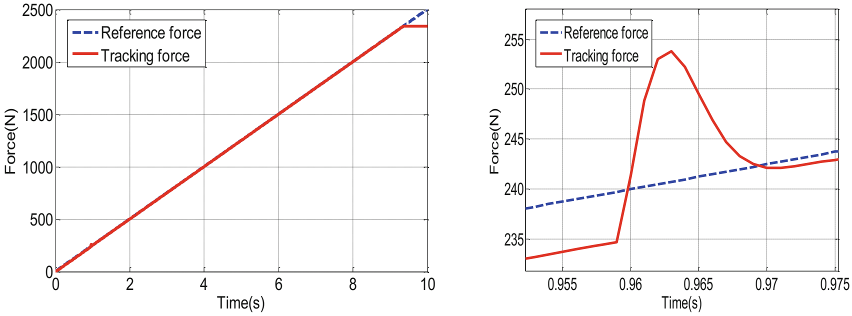

(a)

Fig. 7. Ramp responses for the actuator system. Here, (a) shows the response when both k_1 and k_2 are active, and (b) shows the magnified view when the system switches from the low to the high force situation.

are the natural frequency for the high and the low force respectively. The difference between the natural frequencies is high as the difference between k_1 and k_2 is high, which confirms that the system will not experience resonance either for low force or for high force operation. The frequencies when the magnitudes clearly deviate from zero are about 100 rad/s and 400 rad/s for the low and the high force cases respectively. Again, the frequency when the phase crosses $-180°$ for the low force is about 1500 rad/s (but, the phase does not cross $-180°$ for the high force case). It is seen that 100 rad/s is definitely very smaller than 1500 rad/s, which indicates that the system is stable. Again, the system does not show any tendency of approaching towards 0 dB and $-180°$, which also indicates the stability of the system [36].

$$\omega_{n1} = \sqrt{\frac{k_1}{m_1}} \tag{19}$$

$$\omega_{n2} = \sqrt{\frac{k_2}{m_1 + m_2}} \tag{20}$$

4 Discussion, Conclusions and Future Works

The design of a novel gait rehabilitation system for stroke patients is presented with introduction of its configuration, modules, working methods, actuation, control, novelties etc. The design, configuration, mechanisms, dynamics, control analysis etc. of a novel variable impedance compliant series elastic actuator are presented in details for the rehabilitation system. The dynamic and control characteristics of the actuator in terms of adjustment with sudden disturbances, shocks and impacts (step responses), changes in input with time (ramp responses), stability, absence of oscillations and resonance (bode plots) etc. are proven satisfactory. The actuator is compact, light-weight, it provides variable impedance, compliance, good force controllability,

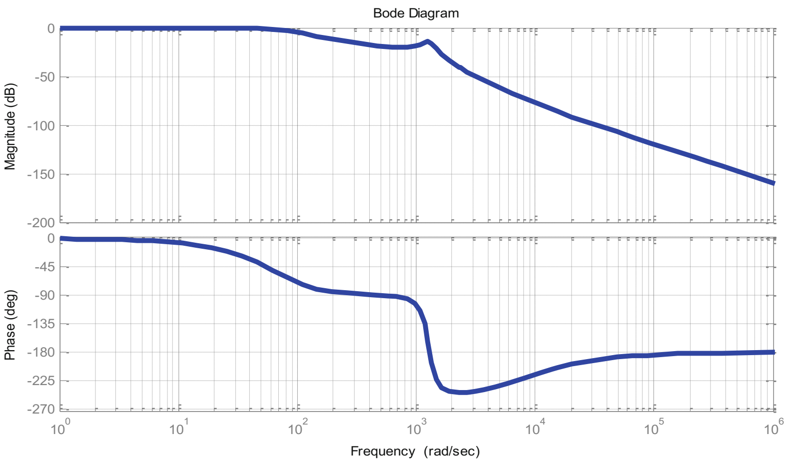

(a)

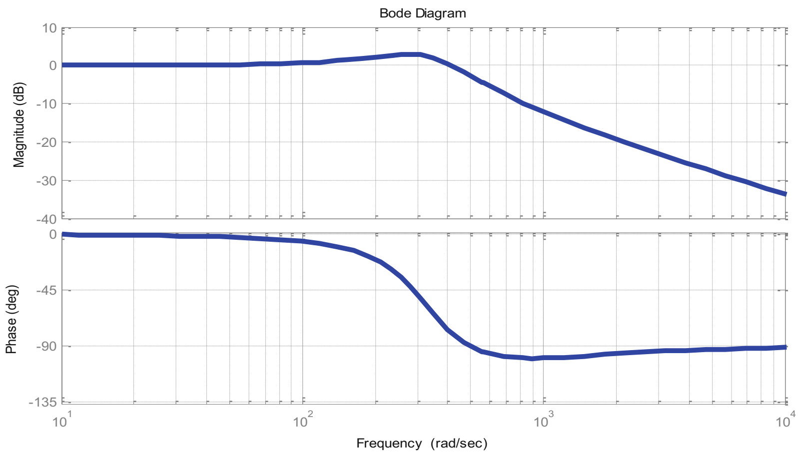

(b)

Fig. 8. Bode plot of the closed-loop control for (a) low force, and (b) high force situation.

back-drivability, large force bandwidths, high efficiency (due to ball screw) and safety, high power/mass and force/mass ratios, high assistive torque etc., and low friction, inertia, impedance etc. These criteria clearly justify the novelties and superiority of the design of the actuator. The rehabilitation system is designed using this novel actuator, and thus the novelties and characteristics of the actuator also benefit the rehabilitation system. The novel actuation strategy along with other novelties such as the advanced materials in construction, adaptive shared control, modularity, omnidirectional mobility, body-weight support, powered ankle, generality, overground application etc. clearly justify the design of the rehabilitation system.

In the future, optimization of the design for static characteristics such as power/energy requirements, kinematic (motion) characteristics of the system etc. will be investigated and compared with human, the fabrication of the rehabilitation system (AFO, KAFO) based on the proposed design will be tried to be finished, an adaptive shared control will be implemented to control the human-robot interactions, and the system will be validated for its each module through clinical trials with stroke patients.

Acknowledgements. The author acknowledges the supports that he received from the National University of Singapore (NUS), Singapore in relation to the work presented in this paper.

References

1. http://www.myheart.org.sg/heart-facts/statistics/
2. Wheeler, J., Krebs, H., Hogan, N.: An ankle robot for a modular gait rehabilitation system. In: Proceedings of the 2004 IEEE/RSJ International Conference on Intelligent Robots and Systems, vol. 2, pp. 1680–1684
3. Brainin, M., Bornstein, N., Boysen, G., Demarin, V.: Acute neurological stroke care in Europe: results of the European stroke care inventory. Eur. J. Neurol. **7**(1), 5–10 (2000)
4. Australian Institute of Health and Welfare.: Heart, stroke and vascular diseases – Australian facts 2004. AIHW Cat. No. CVD 27, Canberra, AIHW and National Heart Foundation of Australia (Cardiovascular Disease Series No. 22)
5. Australian Institute of Health and Welfare.: Secondary prevention and rehabilitation after coronary events or stroke: a review of monitoring issues. AIHW Cat. No. CVD 25, AIHW, Canberra (2003)
6. Turin, T., Kokubo, Y., Murakami, Y., Higashiyama, A., Rumana, N., Watanabe, M.: Lifetime risk of stroke in Japan. Stroke **41**, 1552–1554 (2010)
7. Bharadwaj, K., Hollander, K.W., Mathis, C.A., Sugar, T.G.: Spring over muscle (SOM) actuator for rehabilitation devices. In: Proceedings of the 2004 Annual International Conference of the IEEE Engineering in Medicine and Biology Society, vol. 1, pp. 2726–2729, 1–5 Sept 2004
8. Taub, E., Uswatte, G., Pidikiti, R.: Constraint-induced movement therapy: a new family of techniques with broad application to physical rehabilitation - a clinical review. J. Rehabil. Res. Dev. **36**, vii–viii (1999)
9. Rahman, S., Ikeura, R.: A novel variable impedance compact compliant ankle robot for overground gait rehabilitation and assistance. Procedia Eng. (Elsevier) **41**, 522–531 (2012)
10. Veneman, J., Kruidhof, R., Hekman, E., Ekkelenkamp, R., Van Asseldonk, E.H.F., Van der Kooij, H.: Design and evaluation of the LOPES exoskeleton robot for interactive gait rehabilitation. IEEE Trans. Neural Syst. Rehabil. Eng. **15**(3), 379–386 (2007)
11. Peshkin, M., Brown, D.A., Santos-Munne, J.J., Makhlin, A., Lewis, E., Colgate, J.E., Patton, J., Schwandt, D.: KineAssist: a robotic overground gait and balance training device. In: Proceedings of the 2005 9th IEEE International Conference on Rehabilitation Robotics, pp. 241–246
12. Allemand, Y., Stauffer, Y., Clavel, R., Brodard, R.: Design of a new lower extremity orthosis for overground gait training with the WalkTrainer. In: Proceedings of the 2009 IEEE International Conference on Rehabilitation Robotics, pp. 550–555
13. Zhang, X., Kong, X., Liu, G., Wang, Y.: Research on the walking gait coordinations of the lower limb rehabilitation robot. In: Proceedings of the 2010 IEEE International Conference on Robotics and Biomimetics, pp.1233–1237

14. Yoon, J., Novandy, B., Yoon, C., Park, K.: A 6-DOF gait rehabilitation robot with upper and lower limb connections that allows walking velocity updates on various terrains. IEEE/ASME Trans. Mechatron. **15**(2), 201–215 (2010)
15. Jezernik, S., Colombo, G., Keller, T., Morari, F.: Robotic orthosis lokomat: a rehabilitation and research tool. Neuromodulation **6**(2), 108–115 (2003)
16. Galvez, J.A., Reinkensmeyer, D.J.: Robotics for gait training after spinal cord injury. Technol. Strateg. Enhanc. Mobil. **11**(2), 18–33 (2005)
17. Krebs, H.I., Ferraro, M., Buerger, S.P., Newbery, M.J., Makiyama, A., Sandmann, M., Lynch, D., Volpe, B.T., Hogan, N.: Rehabilitation robotics: pilot trial of a spatial extension for MIT-Manus. J. NeuroEng. Rehabil. **1**, 5 (2004)
18. Nef, T., Mihelj, M., Colombo, G., Riener, R.: ARMin - robot for rehabilitation of the upper extremities. In: Proceedings of the 2006 IEEE International Conference on Robotics and Automation, pp. 3152–3157
19. Lee, C., Seo, K., Oh, C., Lee, J.: A system for gait rehabilitation with body weight support: mobile manipulator approach. J. HWRSERC **2**(3), 16–21 (2000)
20. Vische, D., Kathib, O.: Design and development of high performance torque-controlled joints. IEEE Trans. Robot. Autom. **11**(4), 537–544 (1995)
21. Ferris, D.P., Farley, C.T.: Interaction of leg stiffness and surface stiffness during human hopping. J. Appl. Physiol. (American Physiological Society) **82**, 15–22 (1997)
22. Yang, C., Ganesh, G., Haddadin, S., Parusel, S., Albu-Schaeffer, A., Burdet, E.: Human-like adaptation of force and impedance in stable and unstable interactions. IEEE Trans. Robot. **27**(5), 918–930 (2011)
23. Robinson, D., Pratt, J., Paluska, D., Pratt, G.: Series elastic actuator development for a biomimetic walking robot. In: Proceedings of the 1999 IEEE/ASME International Conference on Advanced Intelligent Mechatronics, pp. 561–568
24. Vallery, H., Veneman, J., Asseldonk, E., Ekkelenkamp, R., Buss, M., Kooij, H.: Compliant actuation of rehabilitation robots. IEEE Robot. Autom. Mag. **15**(3), 60–69 (2008)
25. Tsagarakis, N., Laffranchi, M., Vanderborght, B., Caldwell, D.: A compact soft actuator unit for small scale human friendly robots. In: Proceedings of the 2009 IEEE International Conference on Robotics and Automation, pp. 4356–4362
26. Hirzinger, G., Sporer, N., Albu-Schaffer, A., Hahnle, M., Krenn, R., Pascucci, A., Schedl, M.: DLR's torque-controlled light weight robot III – are we reaching the technological limits now? In: Proceedings of the IEEE International Conference on Robotics and Automation, vol. 2, pp. 1710–1716 (2002)
27. Albu-Schaffer, A., Eiberger, O., Grebenstein, M., Haddadin, S., Ott, C., Wimbock, T., Wolf, S., Hirzinger, G.: Soft robotics. IEEE Robot. Autom. Mag. **15**(3), 20–30 (2008)
28. Schiavi, R., Grioli, G., Sen, S., Bicchi, A.: VSA-II: a novel prototype of variable stiffness actuator for safe and performing robots interacting with humans. In: Proceedings of the 2008 IEEE International Conference on Robotics and Automation, pp. 2171–2176
29. Wolf, S., Hirzinger, G.: A new variable stiffness design: matching requirements of the next robot generation. In: Proceedings of the 2008 IEEE International Conference on Robotics and Automation, pp. 1741–1746
30. Tagliamonte, N.L., Sergi, F., Carpino, G., Accoto, D., Guglielmelli, E.: Design of a variable impedance differential actuator for wearable robotics applications. In: Proceedings of the 2010 IEEE/RSJ International Conference on Intelligent Robots and Systems, pp. 2639–2644
31. Pratt, G., Williamson, M.: Series elastic actuators. In: Proceedings of the IEEE/RSJ International Conference on Intelligent Robots and Systems, vol. 1, pp. 399–406 (1995)

32. Hirai, K., Hirose, M., Haikawa, Y., Takenaka, T.: The development of Honda humanoid robot. In: Proceedings of the 1998 IEEE International Conference on Robotics and Automation, pp. 1321–1326
33. Wassink, M., Carloni, R., Stramigioli, S.: Port-Hamiltonian analysis of a novel robotic finger concept for minimal actuation variable impedance grasping. In: Proceedings of the 2010 IEEE International Conference on Robotics and Automation, pp. 771–776
34. Rahman, S.: A novel variable impedance compact compliant series elastic actuator: analysis of design, dynamics, materials and manufacturing. Appl. Mech. Mater. **245**, 99–106 (2013)
35. Carlson, T., Demiris, Y.: Collaborative control for a robotic wheelchair: evaluation of performance, attention and workload. IEEE Trans. Syst. Man Cybern. B **42**(3), 876–888 (2012)
36. Rahman, S.: A novel variable impedance compact compliant series elastic actuator for human-friendly soft robotics applications. In: Proceedings of the 2012 21st IEEE International Symposium on Robot and Human Interactive Communication, pp. 19–24